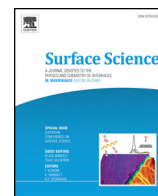




Contents lists available at ScienceDirect

Surface Science

journal homepage: www.elsevier.com/locate/susc

Enhancing the reactivity of gold: Nanostructured Au(111) adsorbs CO

F.M. Hoffmann^a, J. Hrbek^b, S. Ma^b, J.B. Park^{b,1}, J.A. Rodriguez^b, D.J. Stacchiola^b, S.D. Senanayake^{b,*}

^a Department of Science, BMCC-CUNY, New York, NY 10007, USA

^b Department of Chemistry, Brookhaven National Laboratory, Upton, NY 11973-5000, USA

ARTICLE INFO

Available online xxx

Keywords:

CO adsorption
Sputtered Au(111) surface
STM
IRAS
NEXAFS

ABSTRACT

Low-coordinated sites are surface defects whose presence can transform a surface of inert or noble metal such as Au into an active catalyst. Starting with a well-ordered Au(111) surface we prepared by ion sputtering gold surfaces modified by pits, used microscopy (STM) for their structural characterization and CO spectroscopy (IRAS and NEXAFS) for probing reactivity of surface defects. In contrast to the Au(111) surface CO adsorbs readily on the pitted surfaces bonding to low-coordinated sites identified as step atoms forming {111} and {100} microfacets. Pitted nanostructured surfaces can serve as interesting and easily prepared models of catalytic surfaces with defined defects that offer an attractive alternative to vicinal surfaces or nanoparticles commonly employed in catalysis science.

© 2015 Elsevier B.V. All rights reserved.

1. Introduction

Well-prepared atomically flat metal surfaces dominated by large domains of stable crystal faces are not representative of typical surfaces of metal catalysts. Reactivity of fully coordinated atoms present in close-packed structures such as (111) surfaces of fcc metals is often lower than that of steps where metal atoms are low-coordinated [1–6]. Therefore significant research effort is directed towards exploration of surfaces with higher concentration of well-characterized defects found on stepped and vicinal single-crystal surfaces.

Impact of low-energy ions on a surface leads to removal of atoms by a sputtering process [7]. This results in surface roughening and ultimately a spontaneous pattern of pits or ripples develops if a dynamic balance is achieved between the roughening (ion energy and impact angle, ion/sample mass ratio and total ion fluence) and diffusional smoothing (sample temperature and post-annealing) processes. In case of a single-crystalline sample, the shape and morphology of defects reflect the orientation of the sample and its crystallography [8]. The roughened sample surface is healed by heating to temperatures at which the interlayer transport is allowed and the original stable surface is restored.

Gold, highly appreciated by humans for its nobility, is an unlikely candidate as an active catalyst [9,10]. Haruta et al. [11,12] showed that Au is a uniquely active catalyst at low temperatures for selective CO oxidation and interest in exploring gold reactivity has been growing ever since [13]. Surface steps can make a gold (111) surface less noble

as proposed by Mavrikakis et al. [14]. While CO does not adsorb on the Au (111) and (110) surfaces at low pressures and temperatures, its adsorption was reported for the (322) surface [15], (211) stepped single crystal surfaces [16] and for the (111) surfaces structurally modified by ion sputtering [3,17]. Recent work carried out under UHV conditions at very low temperature (30 K) demonstrated CO adsorption on the pristine and on the gold adatoms modified Au(111) surfaces [18].

In the present work, pitted Au surfaces prepared by low-energy ion bombardment of the Au(111) surface, were characterized by STM and the well-defined step sites formed by the process were probed by CO adsorption using IRAS and NEXAFS techniques.

1.1. Experimental methods

Experiments were performed in three separate UHV surface analysis systems for scanning tunneling microscopy (STM), infrared reflection absorption spectroscopy (IRAS) and near edge x-ray absorption fine structure (NEXAFS). The Au(111) surfaces were cleaned by cycles of Ne⁺ sputtering (0.6–1 keV, 2–5 μ A) at room temperature followed by 900 K annealing. The clean gold samples exhibited extended domains of the herringbone reconstruction and no impurities were detectable by XPS or AES. The pitted Au samples were prepared by Ne⁺ sputtering at elevated temperatures (400–450 K) for up to 30 min.

The STM experiments were carried out in a UHV chamber (base pressure 4×10^{-11} Torr) housing a variable temperature STM (Omicron) and LEED. All STM images presented in this work were obtained at room temperature, using the Au(111) single crystal and electrochemically etched tungsten tips [19,20] and processed using the WSxM freeware [21]. The cleaning and preparation of the Au(111) sample took place in an independently pumped preparation chamber attached to the main chamber.

* Corresponding author.

E-mail address: ssenanay@bnl.gov (S.D. Senanayake).

¹ Current Address: Department of Chemistry Education and Institute of Fusion Science, Chonbuk National University, Jeonju 561-756, Republic of Korea.

Infrared reflection absorption spectroscopy (IRAS) [22,23] experiments were performed in a three level UHV surface analysis chamber (base pressure 2×10^{-10} Torr), which contained facilities for IRAS, low energy electron diffraction (LEED), Auger electron spectroscopy (AES) and mass spectroscopy [3]. IR spectra were obtained with a Bruker IFS/66v FTIR spectrometer at a resolution of 4 cm^{-1} at a grazing angle of 85° to the surface normal. Time-evolved temperature-programmed IR spectra were obtained by co-adding 100 scans at time intervals of 40 s. Temperature-programmed IRAS spectra were collected using identical parameters while heating the sample slowly with a linear heating rate of 0.1 K/s. A sample mount allowed cooling to 100 K and heating to 1200 K using a programmable temperature controller. Thermally programmed desorption (TPD) data were collected in a line-of-sight geometry with a UTI-100C mass spectrometer. For preparation of pitted Au(111) the sample was sputtered at elevated temperature without further annealing. After evacuation of neon, the sample was exposed to CO at typ. 5×10^{-9} Torr during cooling to 100 K by backfilling the UHV chamber via a precision leak valve. Exposures are expressed in Langmuirs ($1 \text{ L} = 10^{-6}$ Torr seconds).

NEXAFS experiments were conducted at Brookhaven National Laboratory at the National Synchrotron Light Source (NSLS) in an experimental endstation at beamline U12a. The endstation at this beamline is an ultra-high vacuum (UHV) chamber (1×10^{-10} Torr) equipped with a hemispherical analyzer for XPS, a partial yield electron detector for NEXAFS and all necessary surface science tools for sample preparation [24]. C K-edge NEXAFS was collected with an in-house built PYD detector with a front grid bias of -225 eV and an acceleration voltage of 1800 eV across the single channeltron. The XAS energy calibration is performed using the C features at 284.7 eV corresponding to carbon deposited onto a gold mesh located directly upstream of the endstation. Sample is positioned with an X–Y–Z stage, with sample positioned for analysis with respect to incidence beam and to the PYD detector that is mounted in the same plane. Normal incidence (90°) corresponds to sample positioned normal to the beam, where the energy vector is perpendicular to the surface. Near grazing incidence is with sample at 20° with respect to the incident beam, where the energy vector is parallel to the surface.

2. Results and discussion

2.1. Pitted Au(111)–STM characterization

Depending on specific conditions used during ion bombardment the Au(111) surface can develop a variety of surface morphologies [7]. The critical parameters are sample temperature that affects gold atoms/vacancies' mobility and ion fluence (ions/ m^2) that defines the number of layers removed by sputtering. The resulting morphology is mainly determined by the highest temperature the sample was exposed during or after ion bombardment. Sputtering of gold at room temperature leads to the formation of vacancies, vacancy islands and adatoms on the (111) surface [25,26]. Keeping the sample temperature between 400 and 450 K enhances the mobility of Au vacancies, their annihilation at the steps and diffusion of Au atoms along steps [25], while the structural integrity of gold is preserved as evidenced by the conserved herringbone reconstruction [27]. The Schwebel–Ehrlich barrier prevents interlayer mass transport in this temperature range and the vacancy islands formed by coalescence of individual vacancies have a hexagonal shape with a three-fold symmetry. The vacancy islands are defined by monoatomic steps running in the close-packed $\langle 110 \rangle$ directions of the (111) surface. At higher ion fluences the number of uncovered layers can reach more than 10 and the nested vacancy islands form large areas of nanosized deep pits with a relatively constant pit slope [28–30]. The number of removed layers determines the overall length of the well-defined steps.

In Fig. 1 we show the progression of pit development with increasing ion fluence. When the gold surface is kept at $\sim 400 \text{ K}$ and a low ion

fluence was used, only a small fraction (0.3 layers) of gold surface atoms is removed and the originally smooth surface exposes one layer deep hexagonally shaped vacancy islands of variable sizes, as seen in Fig. 1A. Higher ion fluence that removed 0.6 layers of gold surface atoms, opens new lower layer vacancy islands that have nucleated at the bottom of the existing vacancy islands (Fig. 1B). New individual vacancies created within the existing vacancy islands are not incorporated to ascending steps due to an effective step edge barrier [28]. Their confinement increases the nucleation probability of vacancy islands and leads to pit formation. Individual vacancies formed on narrower terraces between the nested vacancy islands are incorporated into descending steps enlarging the lower layer vacancy islands. Therefore higher layer islands coalesce while new vacancy islands form at the bottom layer of the pit. A dense array of nanosized pits can form on the surface at this stage if the surface terraces are more than 100 nm wide. This is illustrated after additional bombardment and removal of ~ 10 layers of gold surface atoms in Fig. 1C. An array of hexagonal pits consisting of up to 10 stacked vacancy islands separated by ridges with several hexagonal pyramids can be seen.

To evaluate the pitted surface we calculated the Voronoi diagram [31, 32] for the gold surface shown in Fig. 1C. After setting the pits' centers as the sites which partition the surface into regions (Voronoi cells) where each Au atoms inside the cell is closer to this cell site than to any other site. The diagram superimposed on the STM 1C image is shown in Fig. 1D. Thus each Voronoi cell containing a single pit outlines an area from which the Au vacancy had diffused to merge with the growing vacancy island. The mean diffusion length for Au vacancy at 400 K calculated from the diagram is $20 \pm 0.5 \text{ nm}$, and the pits are close-packed with 5.7 ± 0.2 neighbors.

A higher resolution image in Fig. 2A and a line profile of the central deep pit (Fig. 2B) show that the monolayer high steps are separated by about 2 nm (7 to 8 atom) wide (111) terraces. There are about 10^{11} pits/ cm^2 (~ 1000 pits/ μm^2) with average diameter of 14 nm and nearest-neighbor distance of 20 nm; data were obtained from a large scale image shown in Fig. 2C. While the carefully polished and well-prepared surface can have relative density of steps as low as 0.1% the deep-pitted surface shown in Fig. 1C contains about 11% of low-coordinated step atoms.

The 3D STM image in Fig. 3A displays a close up of deep pits, a single layer hexagonal island on the ridge and the herringbone reconstruction of the (111) surfaces between pits (not visible in Fig. 2A). A ball model of the bottom 4 layers of the deep pit (Fig. 3B) shows a local structure of the step edges. On a fcc(111) surface, there are two types of close-packed step edges, denoted A and B. The A-step consists of pseudo-fourfold sites ((100)-microfacet steps), and the B-step consists of pseudo-threefold sites ((111)-microfacet steps). A similar length of A- and B-steps indicates comparable formation energy for both step structures.

2.2. IRAS – adsorption

Vibrational spectra of the adsorption of CO on a Au(111) surface with 8–10 layer deep pits are shown in Fig. 4. The pitted Au(111) surfaces were prepared by Ne^+ ion-sputtering at 400 K, i.e., under conditions, which lead to deep pits as shown in Fig. 2. The time-evolved IRAS spectra in Fig. 4, which were obtained during exposure of the surface to CO at 5×10^{-9} Torr, are characterized by the appearance of a single band at 2124 cm^{-1} . Increasing exposure results in a shift of the C–O stretch frequency from 2124 cm^{-1} to 2114 cm^{-1} and an increase in linewidth from 10 to 12 cm^{-1} (FWHM). The fact that we observe a single band above 2100 cm^{-1} suggests that the CO is linearly bonded, as previously observed for CO adsorbed on polycrystalline Au [33], Au(332) [15], Au(110)–(1×2) [34] and sputtered Au(111) [17].

Details of the adsorption behavior of CO on pitted Au(111) are presented in Fig. 5, which shows a plot of the integrated IR intensities as a function of CO exposure obtained from the spectra in Fig. 4. At

Download English Version:

<https://daneshyari.com/en/article/5421374>

Download Persian Version:

<https://daneshyari.com/article/5421374>

[Daneshyari.com](https://daneshyari.com)